

LU-TP 22-33
June 2022

**On the Energy Dependence of Parameters
in PYTHIA8 Heavy-ion Collision Simulations**

Felipe Abedrapo

Department of Astronomy and Theoretical Physics, Lund University

Bachelor thesis supervised by Leif Lönnblad



LUND
UNIVERSITY

Abstract

Particle collisions are an essential component to the research methodology of particle physics. These investigations are not only conducted in experimental laboratories but also through programs such as PYTHIA that simulate a collision or “event” and then compare its results to known experimental data. This thesis aims to investigate the energy dependence of parameters used in PYTHIA’s Angantyr model for heavy-ion collisions. A significant portion of this project was dedicated to collecting the output of simulated collisions within the energy range of 10 GeV - 10 TeV. The focus was mainly on three parameters in the Angantyr model (k_0 , α , and σ_D) and their parametrizations with respect to the center of mass energy of the collision. This was performed for two versions of Angantyr that differ in the treatment of the opacity of the colliding particles. In the default version a larger particle radius leads to a more opaque particle, and in the second version a smaller radius implies a more opaque particle. It was found that the second version of Angantyr outperformed the default, especially in the low energy range. Additionally, once the functional forms of the relevant parameters of Angantyr were known, they were used to create a Parameterized Energy Dependence (PED) model. It had good agreement with experimental data and therefore the functional forms of the parameters are deemed useful for a possible implementation into PYTHIA.

Popular Science Summary

Particle colliders are the modern “microscopes” that allow us to peer into the most fundamental particles in the universe. These colliders accelerate small particles to very high speeds before having them collide in an area surrounded by detectors. When particles collide at high energies new particles emerge and these new particles, called *final states*, are detected in laboratories. One can acquire insights into the nature of the original particles by investigating where and how many *final states* are detected.

A powerful ally in these investigations are programs that simulate collisions or “events”, and output an estimate of the *final states*. These programs, sometimes called “generators”, are used by physicists to test different models of the collision process and then compare simulation results to real-life experimental data collected in large laboratories. An example of such a program is PYTHIA, and one of its models is called Angantyr. This model has the aim of simulating collisions between heavy-ions (charged particles with multiple protons and neutrons). The purpose of this thesis will be to investigate how certain parameters vary depending on the energy of the collision for different versions of the Angantyr model. The two versions investigated differ in the treatment of the “transparency” of the particle. In the first version a particle, modeled as a disk, becomes more transparent as its size increases. In the second version the opposite is true, with a smaller radius leading to a more transparent disk.

To perform this investigation a large amount of simulations will be run at different energies and their output will be recorded. The acquired information will be used to find suitable equations that describe how the change in energy affects the values of the relevant parameters. Once these dependencies are investigated, comparisons will be made regarding their agreement with experimental data. The final purpose of this thesis is to find equations that model the behaviour of the parameters as simply as possible while maintaining their agreement with real-life data. Finding such a model would prove useful as it could help on deciding which version of Angantyr performs best. It would also serve the purpose of incorporating the parameter equations into PYTHIA, as this would reduce computation time in the simulation.

Contents

1	Introduction	5
2	Theory Background and Method	6
2.1	Overview	6
2.2	pp Collisions in Impact Parameter Space	6
2.3	Angantyr Model for AA Collisions	9
2.4	Method for Simulation Output Collection	11
3	Resulting Parametrizations	12
3.1	Angantyr and PED 1	12
3.2	Distribution of r_s and values of T_0 for PED 1	16
3.3	Angantyr and PED 2	17
3.4	Distribution of r_s and values of T_0 for PED 2	20
4	Conclusions and Outlook	21

List of Figures

1	Scatter plots of Parameters in Angantyr 1 Collision Simulations	13
2	3D Scatter plot of Alpha, Sigma, and Energy for Angantyr 1 Collision Simulations	14
3	Parametrization of α with fixed k_0 and σ_D for Angantyr 1	14
4	Chi-Square Comparison between Angantyr 1 and PED 1 Model	14
5	Cross Sections Comparison for Angantyr 1, PED 1 and the Parametrization of Experimental Data stored in PYTHIA	15
6	PED 1 Distribution of r_s	17
7	PED 1 $E(r_s)$ and its corresponding average T_0 values. The standard deviations of the r_s distribution at different energies are shown as error bars.	17
8	Scatter plots of Parameters in Angantyr 2 Collision Simulations	18
9	3D Scatter plot of Alpha, Sigma, and Energy for Angantyr 2 Collision Simulations	18

10	Parametrization of α with fixed k_0 and σ_D for Angantyr 2	19
11	Chi-Square Comparison between Angantyr 2 and PED 2 Model	19
12	Cross Sections Comparison for Angantyr 2, PED 2, and the Parametrization of Experimental Data	19
13	PED 2 Distribution of r_s	20
14	PED 3 $E(r_s)$ and its corresponding average T_0 values. The standard devi- ations of the r_s distribution at different energies are shown as error bars.	20

List of Tables

1	Values of χ^2 for Angantyr 1 & PED 1	16
2	Values of χ^2 for Angantyr 2 & PED 2	20

1 Introduction

Particle colliders are some of the modern microscopes used to observe fundamental physical processes and test theories and models. Large-scale international laboratories such as the Center for European Nuclear Research (CERN), located in the border between France and Switzerland, accelerate particles to great velocities before colliding them and detecting *final states*, these being the particles that emerge as a result of the collision. The immense amount of data gathered from these experiments can then be used to test models regarding, for example, the interactions of heavy-ions or protons and their constituent partons (quarks and gluons).

With the purpose of studying these interactions a variety of programs that simulate the final states of a collision have been created. These include HERWIG [1], SHERPA [2], and PYTHIA [5], with the latter being the program to be used in this thesis. In the process of simulating a collision event the PYTHIA program has components that have a purely theoretical derivation, while other components have parameters whose values have to be determined using stored experimental data provided by laboratories such as CERN [10]. Monte Carlo methods, which use probability distributions to estimate the values of integrals, are used in event generation as well as parameter tuning and optimization [3]. Both of these are computationally intensive and require extensive run-time. If a process to be studied requires the simulation of multiple collisions at varying energies (a cosmic-ray air shower for example), the calculation and optimization of parameters would have to be performed for every collision energy, thus slowing down the total simulation. This thesis will therefore have the purpose of investigating the energy dependence of parameters, specifically in heavy-ion collisions, with the final aim of providing parametrizations that allow a simulation to quickly obtain the desired values while keeping good agreement between simulation and experimental data.

The framework to be used in PYTHIA is that of the Angantyr model for heavy-ion collisions in which proton-proton (pp) collisions are “stacked” on each other in order to generate a heavy-ion collision event [4]. To set the initial state of the protons there are four parameters whose value needs to be determined: r_0 , k_0 , σ_D and α . The first two parameters can be interpreted as relating to the “size” of the proton while the latter two relate to the “opacity” or “density”. These parameters are used to calculate the probabilities or cross sections of the different kinds of possible interactions.

In section 2 of this thesis there will be an overview of the necessary theory on collisions and particle interaction, such as detailing the Glauber Model [8] and Good-Walker Formalism [7] in subsection 2.2, along with a description of different versions of the Angantyr model in subsection 2.3. Afterwards, the method for obtaining and collecting parameter values for k_0 , σ_D and α is outlined in subsection 2.4. In section 3 the values will be used to create parametrizations and make comparisons between these and Angantyr, specifically in relation to a parametrization of experimental data stored in PYTHIA. Finally, the implications of the energy dependencies observed will be discussed in section 4.

2 Theory Background and Method

2.1 Overview

To understand heavy-ion collisions it is necessary to have a general idea of particle collisions and the PYTHIA simulation program. Collisions between small particles with high energies, or “events”, are commonly treated using the momentum of the colliding particles. In the case of a proton the momentum is divided up among its constituent partons. The fraction of momentum of a given parton and the density function of partons are used by PYTHIA in parton-parton scattering processes, as well its multi-parton interaction (MPI) machinery [3] present in pp and heavy-ion collisions. In such an event, PYTHIA begins by defining the parton density functions and momentum fractions to simulate the event as the sum of many parton-parton interactions.

After this, the Lund String Model is used to begin the hadronization process [11]. In this process the field lines between quarks and gluons that are flying apart begin to resemble strings due to color confinement present in Quantum Chromodynamics (QCD). The strings store more energy as the “tension” of the string increases due to the separation of the quarks. At a certain point the energy is such that random fluctuations lead to the creation of a quark-antiquark pair. These new quarks combine with the initial pair and form hadrons. These hadrons, or the product of their decays, are the simulation’s *final states* and later compared to experimental data.

Nevertheless, when extending the theory from pp collisions to heavy-ions some adjustments need to be made. One such example is that collisions are usually treated in momentum space but when expanding the theory to collisions between two atomic nuclei (AA collisions) it is useful to work instead in the coordinate space of the plane transverse to the trajectory of the particles. This impact-space has an impact parameter denoted by \vec{b} and is used in the Glauber formalism [8], which aims to define the positions of nucleons to be able to understand how many and which nucleon-nucleon subcollisions will occur.

Furthermore, PYTHIA uses the Angantyr model for heavy-ion collisions which relies on the Good-Walker formalism [7] (detailed in section 2.2) to understand diffractive interactions between protons, and the notion of wounded nucleons [9] (detailed in section 2.3) to predict the multiplicity and distribution of final states that will arise due to the collision. The properties of the Angantyr model for heavy-ion collisions will be discussed in following sections with the purpose of investigating the energy dependency of the parameters influencing the model.

2.2 pp Collisions in Impact Parameter Space

A collision between a projectile particle and a target particle can take the particle from an initial state $|i\rangle$ to a final state $|f\rangle$. The probability P_{fi} of this state transition occurring is

calculated using a scattering matrix S where

$$P_{fi} = |\langle f | S | i \rangle|^2 \quad (2.1)$$

and hence for a given initial state $|i\rangle$

$$1 = \sum_f P_{fi} = \sum_f |\langle f | S | i \rangle|^2 = \sum_f \langle i | S^\dagger | f \rangle \langle f | S | i \rangle. \quad (2.2)$$

From the matrix S it is useful to define a transition matrix T as

$$S = 1 - i(2\pi)^4 \delta^4(p_f - p_i) T \quad (2.3)$$

with p_f and p_i being the final and initial momentum respectively, and δ being the Dirac Delta function. This equation can be interpreted as a term that represents no scattering (the 1) followed by a term representing a scattering process occurring [5]. If in a scattering process the final state is the same as the initial state ($f = i$) then it is a forward elastic scattering process.

A quick detour to the optical theorem tells us that the total cross section σ_{tot} of a collision, physically representing an area and in some cases interpreted as a probability, can be related to the elastic scattering amplitude $f(\theta)$ of a wave coming at a scattering angle $\theta = 0$ as

$$\sigma_{tot} = \frac{2\pi}{k} \text{Im}\{f(0)\}. \quad (2.4)$$

It can be shown [6] that using eq. 2.2, replacing S with its definition in eq. 2.3, and approximating the scattering angle θ to 0 for the use of the optical theorem, one can obtain the relations

$$2 \text{Im}\{\langle i | T | i \rangle\} = \sum_f (2\pi)^4 \delta^4(p_f - p_i) |\langle f | T | i \rangle|^2 \quad (2.5)$$

$$\text{Im}\{A_{el}\} = 2s\sigma_{tot} \quad (2.6)$$

where A_{el} is the forward scattering amplitude (originating from the $i \rightarrow i$ transition) and s is the total invariant mass of the collision.

In the case of a collision between two particles it is useful to define both S and T in impact parameter space. This space is the plane transverse to the trajectories of the particles. The collision and scattering amplitudes will now depend on the two-dimensional impact vector \vec{b} representing the distance between the centers of the projectile and target in the transverse plane. Due to the symmetry with respect to the azimuth angle in the collision the vector \vec{b} can be simplified to just a parameter b . In a model where there is only elastic scattering or absorption the elastic amplitude is

$$A_{el}(b) = i(1 - \sqrt{1 - P_{abs}(b)}) \quad (2.7)$$

where P_{abs} is the probability of absorption [6]. The amplitude is then used to define T and S in a similar way as before such that

$$-iA_{el}(b) \equiv T(b) = 1 - S(b). \quad (2.8)$$

Finally with the use of the optical theorem [6] in eq. 2.4 the total and elastic cross-sections are written as

$$\frac{d\sigma_{el}}{d^2b} = |A_{el}|^2 = T^2 \quad \text{and} \quad \frac{d\sigma_{tot}}{d^2b} = 2T \quad (2.9)$$

and hence the inelastic (absorptive) cross section is

$$\frac{d\sigma_{abs}}{d^2b} = \frac{d\sigma_{tot}}{d^2b} - \frac{d\sigma_{el}}{d^2b} = T(2 - T). \quad (2.10)$$

In the case of pp collisions it has to be taken into account that protons have a substructure and are composed of partons in constant fluctuation. The fluctuations can lead to a higher-energy state called diffractive excitation. Therefore within an inelastic collision both diffractive and non-diffractive cross sections should be calculated. In order to do this the Good-Walker formalism is used [7]. In this formalism the mass eigenstate Ψ_i of an incoming particle is a linear combination of the diffractive eigenstates ϕ_k such that

$$\Psi_i = \sum_k c_{ik} \phi_k \quad (2.11)$$

and the amplitude of going from an incoming state i to j is

$$\langle \Psi_j | T | \Psi_i \rangle = \sum_k c_{jk} T_k c_{ik}. \quad (2.12)$$

In an elastic collision the incoming state is the same as the outgoing state ($i = j$). The probability is equal to the square of the amplitude of the wavefunction and likewise to the derivative of the cross section over impact parameter space. Therefore

$$\frac{d\sigma_{el}}{d^2b} = \langle \Psi_i | T | \Psi_i \rangle^2 = \langle T \rangle^2. \quad (2.13)$$

The total diffractive contribution is the sum of the transition from i to all possible excited states j

$$\sum_j |\langle \Psi_j | T | \Psi_i \rangle|^2 = \sum_j \langle \Psi_i | T | \Psi_j \rangle \langle \Psi_j | T | \Psi_i \rangle = \langle T^2 \rangle \quad (2.14)$$

and so to obtain diffractive excitation the elastic cross section is subtracted yielding

$$\frac{d\sigma_{diff}}{d^2b} = \langle T^2 \rangle - \langle T \rangle^2. \quad (2.15)$$

This calculation is performed for the incoming particle (projectile) but in a pp collision both the target and projectile could become diffractively excited. Hence there could be single

diffraction (SD) where only one of particles is diffractively excited and double diffraction (DD). The single diffractive case for a target t is then

$$\frac{d\sigma_{SD}}{d^2b} = \langle\langle T \rangle_t^2\rangle_p - \langle T \rangle_{p,t}^2 \quad (2.16)$$

where $\langle\cdots\rangle_t$ and $\langle\cdots\rangle_p$ means the average over the state of the projectile or target. The case of single diffraction of the projectile p is obtained by switching p and t in the equation. Finally the probability of double diffraction to occur is obtained by taking the total diffractive contribution and subtracting both single diffractive cases

$$\frac{d\sigma_{DD}}{d^2b} = \langle T^2 \rangle_{p,t} - \langle\langle T \rangle_t^2\rangle_p - \langle\langle T \rangle_p^2\rangle_t + \langle T \rangle_{p,t}^2 \quad (2.17)$$

where the last term is the addition of the elastic cross section to compensate for subtracting it in each single-diffractive case. These four cross sections (elastic, absorptive, single diffractive, double diffractive) are important as their values are instrumental in determining the final states of a collision.

2.3 Angantyr Model for AA Collisions

The cross sections will be investigated in this thesis under the framework of the Angantyr model for heavy-ion collisions in PYTHIA. This framework uses the Glauber formalism [8] for extrapolation from pp to pA and AA collisions. An important concept in this formalism is that target nucleons are regarded as independent in pA collisions. The situation is then treated as multiple subcollisions between the projectile proton p and a specific target nucleon N_ν .

Once again it is useful to look at the collision in the coordinate space of the plane transverse to the collision as it is possible to obtain the new scattering matrix $S^{(pA)}$ as the product of the individual S -matrices [4] for each proton-nucleon collision, meaning

$$S^{(pA)} = \prod_{\nu=1}^A S^{(pN_\nu)}. \quad (2.18)$$

Now in each collision there is an impact parameter \vec{b}' dependent on the impact parameter of the projectile \vec{b} and that of the target \vec{b}_ν [5] such that the $\vec{b}' \equiv \vec{b} - \vec{b}_\nu$. The definition for the transition matrix T seen in 2.8 can be inserted into the previous equation yielding

$$T^{(pA)}(\vec{b}) = 1 - S^{(pA)} = 1 - \prod_{\nu=1}^A S^{(pN_\nu)}(\vec{b}') = 1 - \prod_{\nu=1}^A (1 - T^{(pN_\nu)}(\vec{b}')). \quad (2.19)$$

This can be further expanded to collisions between two nuclei A and B where the scattering matrix is given by

$$S^{(AB)}(b) = \prod_{\mu=1}^A \prod_{\nu=1}^B S^{(N_\mu N_\nu)}(b_{\mu\nu}). \quad (2.20)$$

where $b_{\mu\nu}^{\vec{}} \equiv \vec{b}_{\mu} + \vec{b} - \vec{b}_{\nu}$ with \vec{b}_{μ} and \vec{b}_{ν} being the impact parameters for the respective projectile and target nucleons in the subcollision [5]. Using these scattering matrices calculations analogous to that of pp can be performed to obtain the relevant cross sections.

Another important notion is that of wounded nucleons. These are the nucleons that participate in the collision in an inelastic manner [5]. In a first approach these would be the absorbed nucleons, but with the inclusion of the Good-Walker formalism the definition of wounded nucleons is extended to include both absorbed and diffractively excited nucleons. From this definition the cross section for a wounded target nucleon $\sigma_{W,t}$ is therefore

$$\sigma_{W,t} \equiv \sigma_{abs} + \sigma_{SD,t} + \sigma_{DD}. \quad (2.21)$$

Wounded nucleons are important because it has been shown by Bialaz and Czyz [9] that the final state multiplicity distribution can be approximated by

$$\frac{dN}{d\eta} = w_p F(\eta) + w_t F(-\eta) \quad (2.22)$$

where w_p and w_t are the number of wounded projectiles and targets respectively, η is the rapidity, and $F(\eta)$ is a single nucleus emission function. In the case of Angantyr an approximation of the function $F(\eta)$ is made by treating the emissions as that of a single diffractive event. This gives a similar distribution in rapidity and is calculated using PYTHIA's multi-parton interaction model [5].

Within this framework certain assumptions are used to create a model. Colliding nucleons can be modeled as disks because of the length contraction at high velocities. In a first approach the nucleons can be considered black disks with a fixed radius such that any overlap between a projectile and target leads to interaction. In the Angantyr model the disk is grey instead of black and has an 'opacity', meaning that even if there is geometric overlap the interaction is probabilistic. Additionally, there are Gamma-distributed fluctuations in the radius with k_0 and r_0 being the parameters for the distribution [5]. Hence the radius r of a nucleon has a density function

$$P(r) = \frac{r^{k_0-1} e^{-r/r_0}}{\Gamma(k_0) r_0^{k_0}}. \quad (2.23)$$

The elastic amplitude T in a projectile-target collision is dependent on the radius of both nucleons and the impact parameter \vec{b} such that

$$T(\vec{b}, r_p, r_t) = T_0(r_p + r_t) \Theta \left(\sqrt{\frac{(r_p + r_t)^2}{2\pi T_0}} - b \right) \quad (2.24)$$

where r_p and r_t are the radii of the projectile and target respectively [5]. The T_0 term represents the opacity of the disk and is given by

$$T_0(r_p + r_t) = (1 - \exp\{-\sigma_D/\pi(r_p + r_t)^2\})^\alpha. \quad (2.25)$$

Thus there are four relevant parameters r_0 , k_0 , σ_D , and α for the calculations of the matrix T and therefore the cross sections. The parameter r_0 can be analytically calculated from the equation

$$\sigma_{tot} = \int 2T(b, r_p + r_t)P(r_t)P(r_p)d^2bdr_tdr_p \quad (2.26)$$

where $P(r_t)$ and $P(r_p)$ are the probabilities of the Gamma distribution in equation 2.23. One can simplify this equation by using the fact that a sum of two Gamma-distributed $\Gamma(k_0, r_0)$ random variables is itself a Gamma-distributed random variable $r_s \equiv r_p + r_t$ with distribution $r_s \in \Gamma(k_0 + k_0, r_0)$. Thus substituting r_s into equation 2.26 and integrating over b yields

$$\sigma_{tot} = \int r_s^2 P(r_s) dr_s \quad (2.27)$$

which can be read as the expected value of r_s^2 . Using the known Gamma-distribution variance and expected value one can obtain

$$\sigma_{tot} = E(r_s^2) \quad (2.28)$$

$$= Var(r_s) + E(r_s)^2 \quad (2.29)$$

$$= 2k_0r_0^2 + 4k_0^2r_0^2 \quad (2.30)$$

meaning that given a value of k_0 the value of r_0 can be analytically calculated from the known total cross sections as

$$r_0 = \sqrt{\sigma_{tot}/(2k_0 + 4k_0^2)}. \quad (2.31)$$

The other cross sections (Non-Diffractive, Double Diffractive, Wounded Target/Projectile, and Elastic) are not easily written down or solved analytically, and all of them are dependent on the collision energy. Hence a tuning has to be performed to define the parameters in Angantyr at every collision energy. Since r_0 can be calculated from equation 2.31 this thesis will focus on the energy dependence of the remaining three parameters k_0 , σ_D , and α . The relationship will be studied for two different models of Angantyr. In the first model the opacity is given by equation 2.25 whereas in the second model the inverse of the exponent is used, meaning T_0 is calculated as

$$T_0(r_p + r_t) = (1 - \exp\{-\pi(r_p + r_t)^2/\sigma_D\})^\alpha. \quad (2.32)$$

This implies that in the first model an increase in the radii leads to a value of T_0 closer to 0 and therefore a more 'transparent' disk whereas the second model implies that an increase in radii leads to a 'blacker' disk.

2.4 Method for Simulation Output Collection

The Angantyr model uses Monte Carlo integration and a genetic algorithm to define the collision parameters for a given center of mass energy. The genetic algorithm is used to

find parameter values that minimize the difference between simulated cross sections and an energy parametrization of experimental data cross sections stored in PYTHIA, with the difference being quantified as a value using a chi-squared analysis [10]. In each generation of the genetic algorithm 20 points are randomly generated within a bounded 3-dimensional space and the point with the lowest chi-squared value is selected. Then, for each of the remaining 19 points i , a cuboid is created between the selected point and i . The location of point i is then randomized within its corresponding cuboid. Once this is performed for all 19 points a new generation is said to be formed. This method allows for consistent progress towards the minima while allowing for randomness to make a jump between local minima and find the optimal values.

Nevertheless, the inherent randomness present in Monte Carlo and the genetic algorithm creates uncertainty and variation in the calculated parameter values. In large part this is due to an initially created pool of random numbers later used in, for example, Monte Carlo integration. Therefore the pool of random numbers used (otherwise called *seed*) has to be changed in for every run of the program in order to obtain the whole range of possible results at a given energy. The results from various seeds at a given energy are used to parameterize the energy dependence in the 10 GeV - 10 TeV range. From this range 20 energies were selected using logarithmic spacing between them with 100 simulations were run at each energy. It was chosen to use one million integration points for Monte Carlo integration, and 20 generations in the genetic algorithm.

The output of the program was a text file containing the information on the cross sections from experimental data, the resulting cross sections of the simulation, and the resulting parameter values including a chi-square value. These values were stored and later used to observe energy dependencies of the parameters to then parameterize this dependence.

3 Resulting Parametrizations

3.1 Angantyr and PED 1

An early observation was that at low energies the parameter k_0 was too tightly bound by the default maxima set in Angantyr. To allow for an investigation on the full range of energies the maxima were raised for all three parameters to a value high enough such that it did not influence the form of the energy dependence. Figure 1 is obtained by running the collision simulation 100 times with the new maxima at each of the 20 selected energies, and then performing a least-squares fit on the resulting parameter values. After studying the behaviour of the parameters it was chosen to use an exponential decay for k_0 while for σ_D and α a simple 2-degree polynomial was attempted. Hence the parameter equations

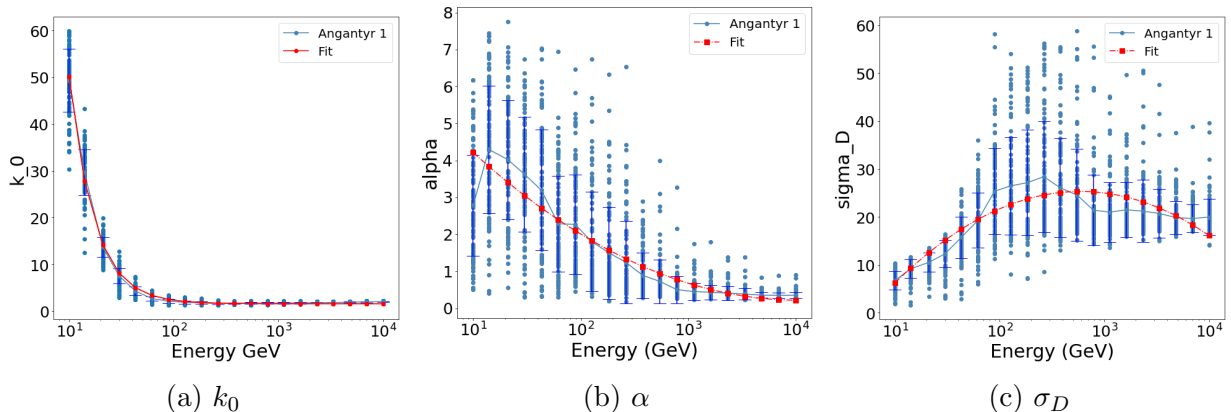


Figure 1: Scatter plots of Parameters in Angantyr 1 Collision Simulations

for a center of mass energy E_{cm} are of the form

$$k_0 = \exp\{-a_1 (\log(E_{cm}) - b_1)\} + c_1 \quad (3.1)$$

$$\alpha = a_2(\log E_{cm})^2 + b_2(\log E_{cm}) + c_2 \quad (3.2)$$

$$\sigma_D = a_3(\log E_{cm})^2 + b_3(\log E_{cm}) + c_3 \quad (3.3)$$

with $a_1 = 1.82$, $b_1 = 4.44$, and $c_1 = 1.63$ for k_0 . Since σ_D and α are much more interconnected (both relate to the 'opacity') and their fits less accurate it was decided to use set k_0 values according to its parametrization and move on to finding relations between the other two variables. This is done with the intention of reducing the number of coefficients for α and σ_D .

The 3D plots in Figure 2 were used to observe the relationship between α , σ_D and the logarithm of the energy. In the top-view one can see that a vertical line at $\sigma_D = 13.5$ crosses a point for almost any value of α . This implies that there was a minima found with that (α, σ_D) pair. Additionally the color range goes from the low-energy purple to the high-energy yellow, meaning an (α, σ_D) configuration should exist for every energy in the range, thus giving further motivation for the selection of σ_D .

Once this value for σ_D was selected the program was run 50 times at each of the 20 energies, this time setting k_0 fixed according to its value given by its parametrization (eq. 3.1) and having $\sigma_D = 13.5$. The resulting energy dependency of α , the only variable parameter left, is seen in Figure 3. An exponential fit of the same form as in eq. 3.1 was performed yielding values $a_1 = 1.088$, $b_1 = 4.728$ and $c_1 = 0.025$ for α .

The use of these resulting parametrizations to set the values for k_0 , σ_D and α when running Angantyr collision simulations in PYTHIA will be called Parameterized Energy Dependence (PED) and referenced as PED 1 or 2, depending on the Angantyr model used to create it. In Figure 4 one can observe the differences in the chi-squared value output by PYTHIA when running Angantyr 1 and PED 1. This is not to be interpreted as a comparison of quality but instead as a check to be assured that PED 1 yields similar re-

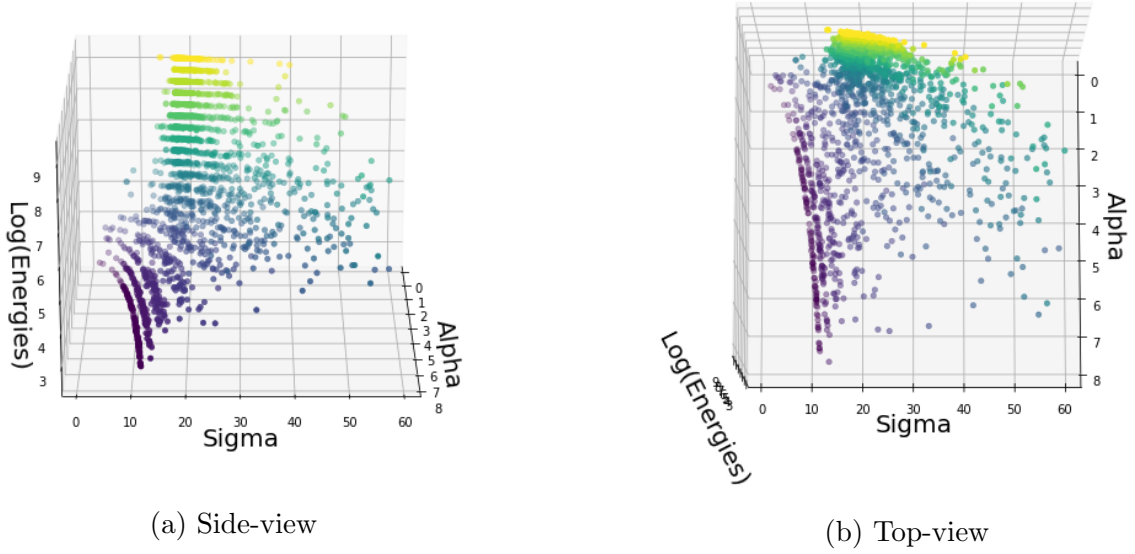


Figure 2: 3D Scatter plot of Alpha, Sigma, and Energy for Angantyr 1 Collision Simulations

sults as Angantyr 1. It is therefore also central to observe the cross sections and check for agreement with the energy parametrization of experimental data stored in PYTHIA (referenced as Experimental Data for conciseness in Figure 5 and the rest of this thesis). These are seen in Figure 5, with the most relevant ones being the Wounded Target as calculated in eq. 2.21 (in this case the target and projectile have the same cross section) and Non-Diffractive (absorptive), as these are the ones with the largest cross sections and drive the results of the final states.

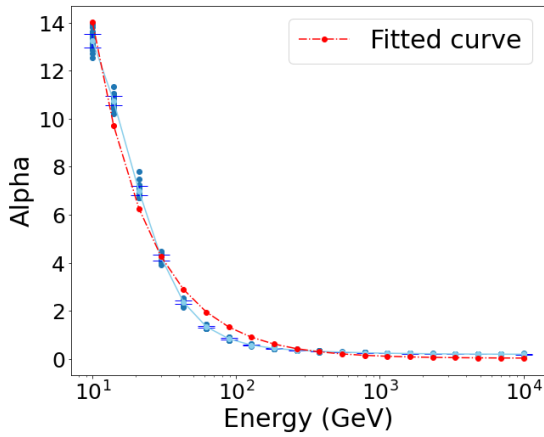


Figure 3: Parametrization of α with fixed k_0 and σ_D for Angantyr 1

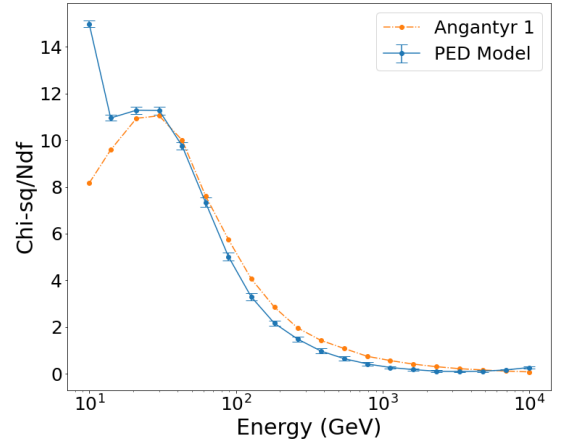


Figure 4: Chi-Square Comparison between Angantyr 1 and PED 1 Model

An analysis of the quality of the fit between the data and the simulation or model can be

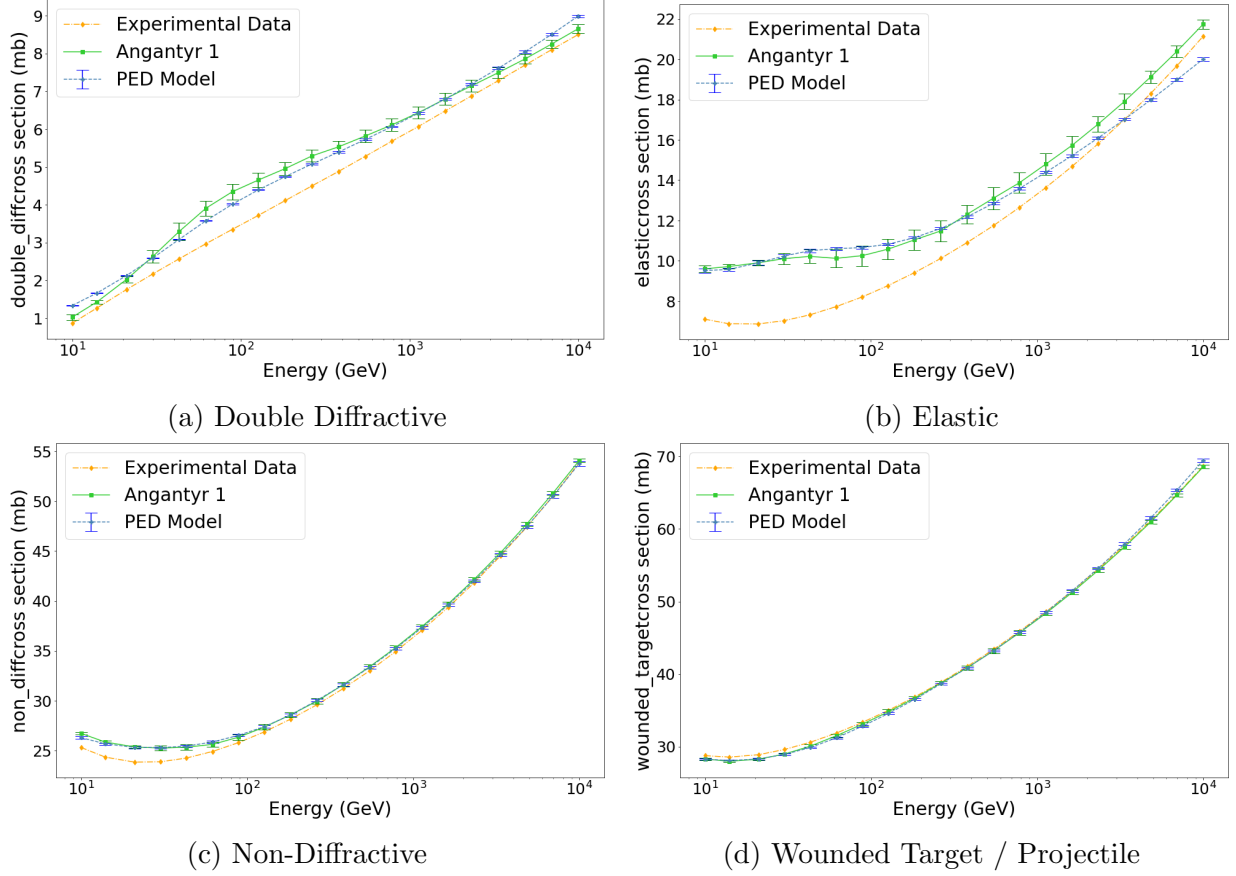


Figure 5: Cross Sections Comparison for Angantyr 1, PED 1 and the Parametrization of Experimental Data stored in PYTHIA

performed using the equation

$$\chi^2 = \sum_{i=1}^{20} \left(\frac{\sigma_i - \sigma_{data,i}}{\epsilon \cdot \sigma_{data,i}} \right)^2 \quad (3.4)$$

where σ_i is the average cross section value for the i th energy in the model, $\sigma_{data,i}$ is the experimental data cross section, and ϵ is the assumed percentage error of $\sigma_{data,i}$ as stated in Angantyr ¹. The χ^2 value for both Angantyr and PED are summarized in Table 1. Given the proximity of the χ^2 values between Angantyr and PED, along with the visual similarity in Figure 5, it can be stated that the choice and results of the parametrizations for k_0 , α , and σ_D are reasonable. The advantage of PED comes in when looking into the degrees of freedom. In both Angantyr and PED there were 20 energies selected for each of the four cross sections, meaning 80 data points. In Angantyr there are 3 free parameters

¹The stated error is not necessarily experimental error. It is instead an indication of the relevance of the cross sections for final state calculations, with the most important cross sections having the smallest error percentage. They can be seen in Table 1.

Cross Section	ϵ	Angantyr	PED
Elastic	10%	123.3	113.7
Double Diffractive	10%	70.2	56.4
Wounded Target	5%	1.33	0.90
Non-Diffractive	2%	44.6	47.8

Table 1: Values of χ^2 for Angantyr 1 & PED 1

(k_0, α, σ_D) for each of the 20 energies whereas PED uses 6 free parameters (the respective a, b , and c for k_0 and α) for the whole energy range. In total this means that Angantyr has $80 - 60 = 20$ degrees of freedom while PED has $80 - 6 = 74$ degrees of freedom.

3.2 Distribution of r_s and values of T_0 for PED 1

Both r_p and r_t are $\Gamma(k_0, r_0)$ -distributed. As done in the calculation of r_0 (eq. 2.27) it is useful to combine r_p and r_t into one variable $r_s \equiv r_p + r_t$ with distribution $\Gamma(2k_0, r_0)$. One can begin to understand how the distribution of r_s varies with respect to the collision energy by observing the energy dependency of k_0 . Using the known parametrization of k_0 in PED 1 and knowing that the remaining parameter r_0 can be calculated using equation 2.31, it is possible to observe the change in the distribution at varying energies in Figure 6.

At low energies the distribution is narrower, implying less fluctuations in the radius of the nucleons. This follows one's intuition in which less availability of energy would lead to less deviation from the average state. It is likewise interesting to observe the change in r_0 . An important feature of the distribution that encompasses both these changes is the expected value since $E(r_s) = k_0 \cdot r_0$ and $Var(r_s) = k_0 r_0^2$. From the expected value of r_s , the fixed σ_D , and the parametrization of α it is possible to calculate the average 'opacity' T_0 from eq. 2.25 and whose results are seen in Figure 7.

In the range 10 GeV - 100 GeV the expected value of r_s stays relatively constant with a small standard deviation shown as error bars, while in the range 100 GeV - 10 TeV there is a linear behaviour together with an increase in standard deviation as expected from a wider distribution. This, in combination with the exponential nature of α (with respect to the logarithm of the energy) seen in Figure 3 serves as an explanation for the behaviour of T_0 . Until energies below 1000 GeV T_0 is driven by the high value of α . Once α flattens out the change in T_0 is caused by the increase in r_s . This second effect is much more subtle but it can be seen that there is a small decrease in T_0 between $10^3 - 10^4$ GeV. This behaviour is expected in Angantyr 1 because, as seen in eq. 2.25, an increase in the radius of the disk would lead to the disk being more transparent.

The value of T_0 is concerning in the low energy range as it goes to 0. This could've been expected already from Figure 10 due to high value of alpha for energies below 100 GeV.

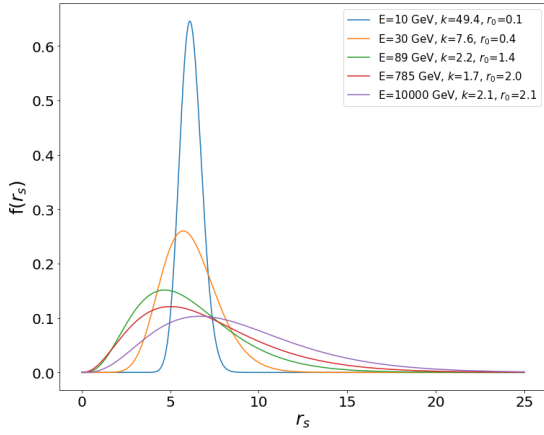


Figure 6: PED 1 Distribution of r_s

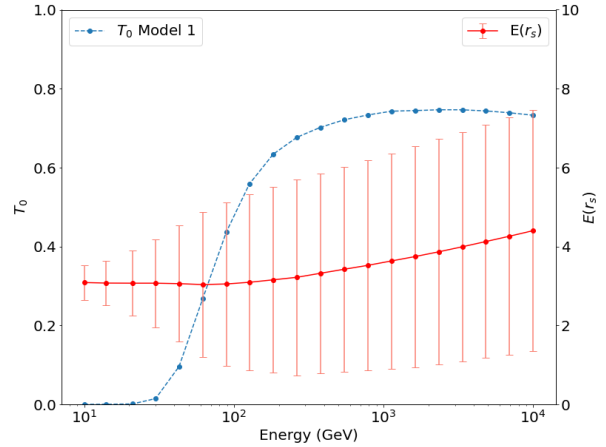


Figure 7: PED 1 $E(r_s)$ and its corresponding average T_0 values. The standard deviations of the r_s distribution at different energies are shown as error bars.

In the calculation of T_0 (eq. 2.25), α is an exponent to a number that is bounded between 0 and 1. Therefore T_0 will approach 0 for large enough values of α regardless of the value of σ_D or r_s . This explains the large variation of k_0 in its original scatter plot in Figure 1a as its value becomes less relevant to the cross sections. There is also a noticeable visual discrepancy of the cross sections in the low energy range (especially in the elastic one) and the T_0 behaviour also helps explain the spike in values of chi-squared observed in this range. Overall this points to an unstable behavior by Angantyr 1 & PED 1, thus opening avenues for other versions of the model.

3.3 Angantyr and PED 2

As in the case of Angantyr 1, 100 collision events were simulated at each of the 20 energies for Angantyr 2, with the resulting data points and respective fits for the parameters being seen in Figure 8. In order to create parametrizations a similar process was performed for this second model. The exponential functional in eq. 3.1 was used for k_0 again, now yielding values $a_1 = 3.17$, $b_1 = 2.9$, and $c_1 = 1.5$. In Angantyr 2 the scatter plots for both σ_D and α seem to be linear and have large standard deviations. Therefore k_0 will once again be used as the basis for the parametrization of σ_D and α .

From the 3D plots in Figure 9 it is clear there exists an interconnection between α and σ_D along with the fact that they can 'compensate' for each other since both relate to opacity. For this reason it is possible to set one of the parameters fixed and let the other one vary between generations of the genetic algorithm with the purpose of finding its optimal value. It was chosen to take σ_D as the fixed parameter at its average of 12.44 as calculated from the data points visualized in Figure 8b.

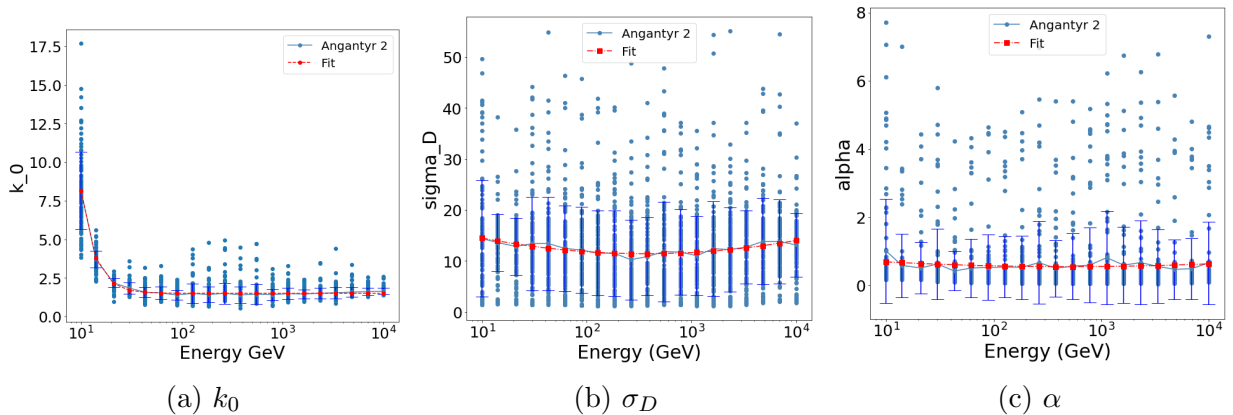


Figure 8: Scatter plots of Parameters in Angantyr 2 Collision Simulations

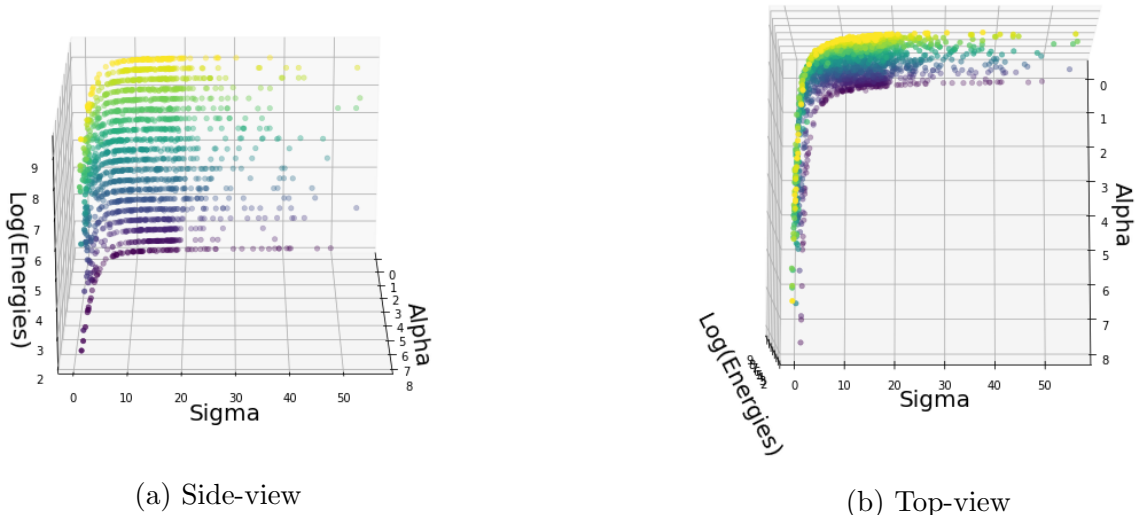


Figure 9: 3D Scatter plot of Alpha, Sigma, and Energy for Angantyr 2 Collision Simulations

With the value of k_0 being fixed according to its parametrization and with $\sigma_D = 12.44$, the simulation was run 50 times at each of the 20 energies. This yielded an energy-dependency relation for α seen in Figure 10. The fit chosen was quadratic of the form $\alpha = a(\log E_{cm})^2 + b \log E_{cm} + c$, with the least-squares method giving the values $a = 0.0149$, $b = -0.188$, and $c = 0.734$. The chi-square comparison is seen in Figure 11 and implies reasonable agreement between PED 2, Angantyr 2, and the parametrization of experimental data due to the low chi-squared values.

The agreement can be visually corroborated by plotting the cross sections. Once again the Non-diffractive and the Wounded Target cross sections dominate the final states calculations by having the largest cross sectional values. Additionally they have the best agreement with the parametrization of experimental data. It should be noticed as well

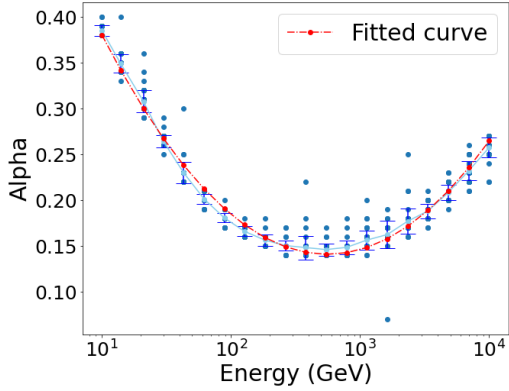


Figure 10: Parametrization of α with fixed k_0 and σ_D for Angantyr 2

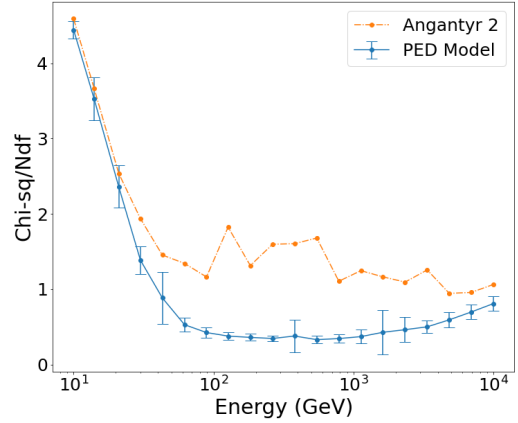
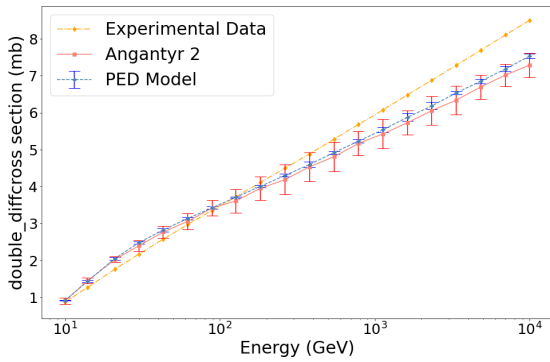
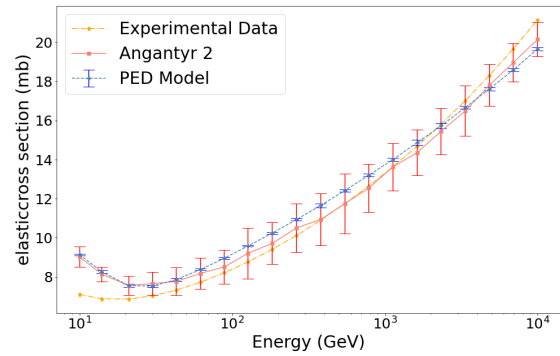


Figure 11: Chi-Square Comparison between Angantyr 2 and PED 2 Model

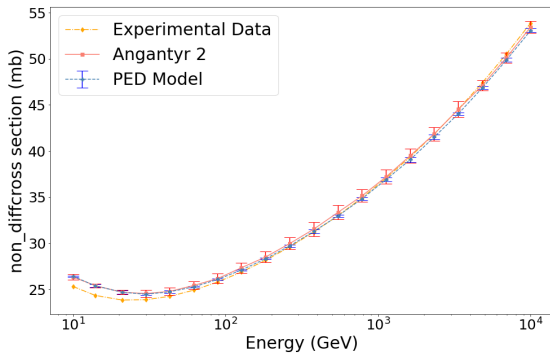
that there is an important improvement in the elastic cross section in relation to Angantyr 1 as seen in Figure 12.



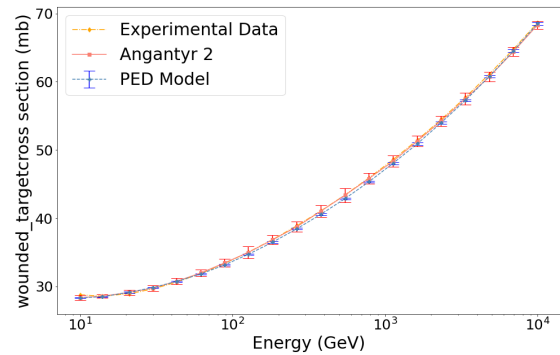
(a) Double Diffractive



(b) Elastic



(c) Non-Diffractive



(d) Wounded Target / Projectile

Figure 12: Cross Sections Comparison for Angantyr 2, PED 2, and the Parametrization of Experimental Data

A further error analysis can be performed once again using eq. 3.4 and the results can be seen in Table 2.

Cross Section	ϵ	Angantyr	PED
Elastic	10%	20.1	14.4
Double Diffractive	10%	17.24	20.14
Wounded Target	5%	0.64	0.20
Non-Diffractive	2%	18.18	19.45

Table 2: Values of χ^2 for Angantyr 2 & PED 2

3.4 Distribution of r_s and values of T_0 for PED 2

Given the agreement between PED 2 and experimental data it is reasonable to calculate the distribution of r_s and the energy dependence of the average T_0 exhibited by PED 2. The distribution for r_s is seen in Figure 13, while the dependence of T_0 , calculated using the parameterized values of k_0 , α , σ_D , and the average r_s , is shown in Figure 14.

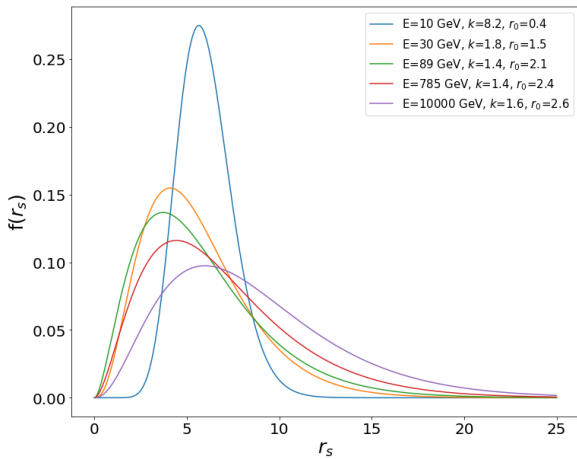


Figure 13: PED 2 Distribution of r_s

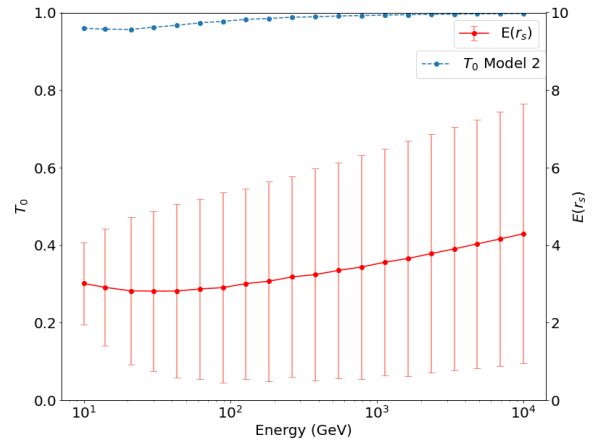


Figure 14: PED 3 $E(r_s)$ and its corresponding average T_0 values. The standard deviations of the r_s distribution at different energies are shown as error bars.

Once again the distribution of r_s in the low energy range is characterized by a smaller spread and hence less fluctuations from the mean as visualized by the error bars calculated from the standard deviation of the distribution. The behaviour of $E(r_s)$ in this model is similar to that of PED 1. An important difference lies in the value of the average T_0 . It begins at a value very close to 1 and further approaches it as the energy increases. A T_0 value of 1 means a black disk model, and the results from PED 2 would imply that this model could be quite useful for the calculation of the cross sections. Overall it can

be concluded that both models have similar performance in the high energy range, but Angantyr and PED 2 perform much better in the low energy range due to the unstable nature of the first model, and therefore Angantyr 2 and PED 2 are to be preferred.

4 Conclusions and Outlook

The most important conclusion from the conducted investigation is the relationships between the parameters k_0 , α , and σ_D and the center of mass energy in heavy-ion collisions. This was performed for both Angantyr 1 and Angantyr 2 frameworks in PYTHIA. From these parametrizations PED 1 and 2 were created and their relevant features investigated in the 10 GeV - 10 TeV energy range.

For both Angantyr 1 and 2 it was found that k_0 had an exponential relation to the logarithm of the energy. Its final parametrization is of the form

$$k_0 = \exp\{-a(\log(E_{cm}) - b)\} + c. \quad (4.1)$$

Using k_0 as a basis it was chosen to fix σ_D at a constant value for the whole energy range. Afterwards the energy dependency of α was once again investigated, and found to have an exponential relation to the logarithm of the energy for Angantyr 1 and a quadratic relation for Angantyr 2. The agreement between the cross sections in Angantyr 1, PED 1, and the experimental data was observed visually and statistically with reasonable agreement being found, especially in the high energy range 1 TeV - 10 TeV. Angantyr 2 and PED 2 had a similar agreement in the high energy range but a clear improvement in performance in the low 10 GeV - 100 GeV range.

The Gamma distribution of the sum of the 'radii' of the projectile and target was summarized in a variable r_s and calculated. At lower energies the spread of the distribution was narrower, implying that higher energies lead to greater fluctuations from the mean for both PED 1 and 2. A less intuitive result was that the expected value of r_s increased exponentially with respect to the energy in the energy range 100 GeV - 10 TeV for both models as well. These values were used to investigate the behavior of the opacity T_0 of the disks.

The average T_0 value for PED 1 had an almost logistic distribution with respect to the logarithm of the energy and flattened out at approximately 0.7 in the 1 TeV - 10 TeV range. In the low energy range (10 GeV - 100 GeV), the value of T_0 was unstable and went down to almost 0 due to the large values of α . This would imply an almost completely transparent and non-interacting disk, which would explain why there is a larger deviation between experimental and simulated cross sections in the low energy range. On the other hand, PED 2 had an average T_0 value consistently close to 1, and even approaches it further as energy increases. A value of 1 for T_0 means the disk representing the particle is completely black, and the results from PED 2 implies that this approximation would be a useful one for the purpose of calculating cross sections.

A first important outlook for this thesis would be the change in the default model of Angantyr in PYTHIA, as there was closer agreement to experimental data in Angantyr 2 (especially in the low energy range). Additionally, the physical implications of Angantyr 1 & PED 1 in the low energy range is that of an almost completely transparent disk, which is not very reasonable, thus giving more support to the use of Angantyr 2 & PED 2 over it.

Although there was a lot of focus in finding the specific parametrizations of k_0 , α , and σ_D using the least degrees of freedom possible, the potential lies not on the specific values but instead on the form of the energy dependence. When considering a process with many collisions at different energies, such as a cosmic-ray air shower, it is useful to know the behaviour of the parameters in that energy range. One can then use the form of the energy dependence to calculate parameter values over a range instead of having to perform a new calculation at every energy involved, thus being more computationally and time efficient. Therefore, by knowing the functional form of the parameters, a fit could be created and used for an energy range when initializing the simulation program. Due to the good agreement between experimental cross sections and those in PED 2 its functional forms for the parameters could be implemented in future versions of PYTHIA.

References

- [1] Marchesini, G., Webber, B., Abbiendi, G., Knowles, I., Seymour, M. and Stanco, L., 1992. HERWIG 5.1 - a Monte Carlo event generator for simulating hadron emission reactions with interfering gluons. *Computer Physics Communications*, 67(3), pp.465-508.
- [2] Höche, S., Maierhöfer, P., Moretti, N. et al, 2017. Next-to-leading order QCD predictions for top-quark pair production with up to three jets. *Eur. Phys. J. C* 77, 145. <https://doi.org/10.1140/epjc/s10052-017-4715-y>
- [3] Sjöstrand, T., Ask, S., Christiansen, J., Corke, R., Desai, N., Ilten, P., Mrenna, S., Prestel, S., Rasmussen, C. and Skands, P., 2015. An introduction to PYTHIA 8.2. *Computer Physics Communications*, 191, pp.159-177, arXiv:1410.3012v1.
- [4] Bierlich, C., Gustafson, G. and Lönnblad, L., 2016. Diffractive and non-diffractive wounded nucleons and final states in pA collisions. *Journal of High Energy Physics*, 2016(10).
- [5] Lönnblad, L., Bierlich, C., Gustafson, G., and Shah, H., 2018. The Angantyr model for Heavy-Ion Collisions in PYTHIA8. *Journal of High Energy Physics*, 134.
- [6] Bierlich C., 2017. Rope Hadronization, Geometry and Particle Production in pp and pA collisions, PhD Thesis, Lunds Universitet, Lund.
- [7] Good, M. and Walker, W., 1960. Diffraction Dissociation of Beam Particles. *Physical Review*, 120(5), pp.1857-1860.
- [8] Miller, M., Reygers, K., Sanders, S. and Steinberg, P., 2007. Glauber Modeling in High-Energy Nuclear Collisions. *Annual Review of Nuclear and Particle Science*, 57(1), pp.205-243.
- [9] Bialas, A. and Czyz, W., 2005. Wounded nucleon model and Deuteron-Gold collisions at RHIC, *Acta Phys. Polon.* B36 905 [hep-ph/0410265].
- [10] C. Bierlich, T. Sjöstrand, L. Lönnblad, et al. "A comprehensive guide to the physics and usage of PYTHIA 8.3" <https://arxiv.org/pdf/2203.11601.pdf>
- [11] Andersson, B., Gustafson, G., Ingelman, G. and Sjöstrand, T., 1983. Parton fragmentation and string dynamics. *Physics Reports*, 97(2-3), pp.31-145.